JOURNAL OF SOLID STATE CHEMISTRY **121,** 273–277 (1996)
ARTICLE NO. 0038

# Crystal Growth, Electrical, and Magnetic Properties of Niobium Phosphate Bronze: $Na_{2+x}P_4Nb_6O_{26}$

J. Xu and M. Greenblatt[1]

*Chemistry Department, Rutgers, The State University of New Jersey, Piscataway, New Jersey 08854*

Received May 23, 1995; in revised form October 3, 1995; accepted October 5, 1995

**Large single crystals of the bronze $Na_{2+x}P_4Nb_6O_{26}$ were grown by chemical vapor transport technique with either $NH_4Cl$ or NaCl as the transporting agent. The directional electrical transport properties along the three orthorhombic crystallographic axes show anisotropic semiconducting behavior with the activation energies of 0.13, 0.15, and 0.12 eV for $E_a$, $E_b$, and $E_c$, respectively. Magnetic susceptibility measurements indicate Curie–Weiss behavior with $\mu_{eff} = 1.14\ \mu_B/Nb^{4+}$.** 

## INTRODUCTION

A wide variety of transition metal phosphate bronzes have been synthesized in the past 20 years because of their potentially interesting physical properties, including anisotropic electrical transport, magnetic properties, charge-density-wave (CDW) driven metal–semiconductor transition (1), and shape-selectivity (2). The characteristic building units of transition metal phosphate bronzes are conducting chains/layers of $MO_6$ octahedra (where $M$ can be Ti, V, Nb, Mo, or W (3, 4)), separated by insulating chains/layers of $PO_4$ tetrahedra. These highly anisotropic structural features of the transition metal phosphate bronzes give rise to highly anisotropic physical properties. When $M$ is W, for example, in $(PO_2)_4(WO_3)_{2m}$, the monophosphate tungsten bronzes with pentangonal tunnels ($MPTB_p$), the $m = 2$ member, $PWO_5$, shows highly anisotropic semiconducting behavior in the temperature range $10 \sim 390$ K and the magnetic susceptibility measurements indicate Curie–Weiss behavior with an antiferromagnetic ordering at ~15 K (5), while the $m = 4, 6$, and 7 members of the $MPTB_p$ are metallic at room temperature and undergo multiple CDW transitions at low temperature (1). In the $MPTB_p$'s probably, because of the severe distortion of the $ReO_3$-type slabs of $WO_6$ to accommodate the interconnecting layers of $PO_4$ tetrahedra the $m = 3$ member of the $MPTB_p$ family, "$P_4W_6O_{26}$" could not be prepared so far. However, the isostructural $m = 3$ phase of the niobium analog of $MPTB_p$ $(Na_x(PO_2)_4(NbO_3)_{2m})$ $Na_{2+x}P_4Nb_6O_{26}$ $(0 < x < 0.75)$ was recently synthesized by Benabbas *et al.* (6). They obtained small, dark-blue single crystals of $Na_{2.66}P_4Nb_6O_{26}$ by a solid state reaction and determined its structure by single crystal X-ray analysis. The framework of $Na_{2+x}P_4Nb_6O_{26}$ is built up of $NbO_6$ octahedra cornersharing in a zig-zag fashion along the $a$ axis; along the crystallographic $b$ direction these $NbO_6$ chains are connected by $PO_4$ tetrahedra. This arrangement of the polyhedra network gives rise to an anisotropic structure (6). However, no physical properties of the compound have been reported so far. In order to investigate the anisotropic physical properties of this compound, relatively large single crystals of $Na_{2+x}P_4Nb_6O_{26}$ are essential.

In this paper we report single crystal growth and characterization of the electrical transport and magnetic properties of oriented single crystals of $Na_{2+x}P_4Nb_6O_{26}$. A comparison of the physical properties of $Na_{2+x}P_4Nb_6O_{26}$ with related tungsten phosphate bronzes and other niobium phosphate bronzes is also presented.

## EXPERIMENTAL

Single crystals of $Na_{2+x}P_4Nb_6O_{26}$ were grown in two steps. Initially a starting mixture of $Na_2CO_3$ (Fisher, A. C. S grade), $(NH_4)_2HPO_4$ (Fisher, A. C. S grade), and $Nb_2O_5$ (Alfa, 99.5%) in the composition of $Na_3P_4Nb_{5.6}O_{26}$ was heated in a porcelain crucible in air at 600°C to decompose the carbonate and phosphate. An adequate amount of metal niobium (Johnson Matthey electronics, 99.98%) and either $NH_4Cl$ or NaCl (5% in mole) (Fisher, A. C. S grade) were mixed with the $Na_3P_4Nb_{5.6}O_{26}$ precursor to reach the composition of $Na_3P_4Nb_6O_{26}$; the mixture was thoroughly ground, pelletized, sealed in an evacuated quartz tube, and heated for a week at 1150°C. A quartz tube about 15 cm long with 1.0 cm i.d. and 1.2 cm o.d. was charged with about 0.5 gram of reactant mixture and placed in a muffle furnace horizontally such that a temperature gradient about 30°C developed along the length of the tube. The cooling rate was 10°C/hr to 1000°C followed by 20°C/hr

[1] To whom correspondence should be addressed.



0022-4596/96 $18.00

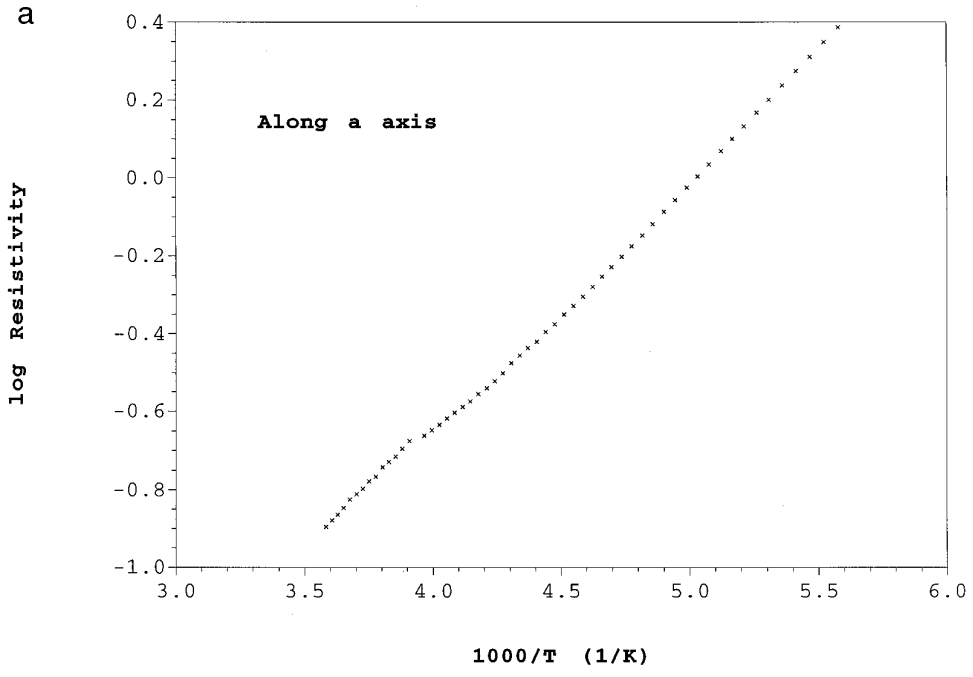


**FIG. 1.** The temperature dependence of log $\rho$ for $Na_{2.63}P_4Nb_6O_{26}$ along the three orthorhombic crystallographic axes, *a*, *b*, and *c*.

to 500°C; then the tube was quenched in air. The corresponding bronzoid (i.e., the fully oxidized form) $Na_2P_4Nb_6O_{26}$ was prepared according to the method of Benabbas *et al.* (6).

The powder X-ray diffraction patterns (PDX) were recorded with a Scintag PAD V X-ray diffractometer with Cu$K\alpha$ radiation. Silicon powder was used as an internal standard. The least-squares program (LATCON) was used for indexing the PXD. The orientation of the crystal axes was determined by oscillation and Weissenberg photographs.

Electrical resistivity measurements on selected crystals ($\sim 1.2 \times 0.8 \times 2.5$ mm$^3$ size) were made by a standard four-probe technique along the *a* and *c* axes with a Displex Cryostat (APD cryogenics, model DE 202) in the temperature range 300–140 K. Due to the small thickness of the plate-like crystals, only room temperature resistivity was measured along the *b* axis in a four probe configuration (i.e., manually contacting the crystal). The resistivity as a function of temperature along the *b* axis was measured by a two probe technique. Indium leads were attached to the appropriate crystal faces with a silver print. The I–V profiles were recorded at different temperatures to ensure the Ohmic nature of the contacts.

The magnetic susceptibility data were recorded with a Quantum Design SQUID magnetometer in the temperature range 2.5–300 K on a collection of randomly oriented single crystals. The applied magnetic field was 0.5 T and corrections for the core diamagnetism contribution of the component ions were applied.

Elemental analysis was performed by the electron microprobe technique (JEOL. JXA-8600 Superprobe) and inductive coupled plasma spectroscopy (Plasma 400, Perkin Elmer Co.).

**TABLE 1**
**The Cell Parameters of Bronzes $Na_{2+x}P_4Nb_6O_{26}$ and the Bronzoid $Nb_2P_4Nb_6O_{26}$**

| Sample | *a* (Å) | *b* (Å) | *c* (Å) |
|---|---|---|---|
| $Na_{2.66}P_4Nb_6O_{26}$ (Reported) | 19.805(1) | 14.3859(7) | 5.3960(4) |
| $Na_{2.63}P_4Nb_6O_{26}$ (This work) | 19.854(3) | 14.434(3) | 5.4166(10) |
| $Na_2P_4Nb_6O_{26}$ (This work) | 19.801(4) | 14.403(3) | 5.391(1) |

## RESULTS AND DISCUSSION

Large single crystals of $Na_{2+x}P_4Nb_6O_{26}$ were grown by a method similar to that used for $K_3P_4Nb_6O_{26}$ (7). Without the chemical transport agents, the reactant mixture melted completely upon heating and single crystals did not form. However, when 5% (by mole) of $NH_4Cl$ or NaCl was charged into the reactant mixture, well-formed, up to $1.2 \times 0.8 \times 2.5$ mm$^3$ dark-blue plate crystals of $Na_{2+x}P_4Nb_6O_{26}$ were obtained at the cool end of the tube. The crystal size improved with annealing time.

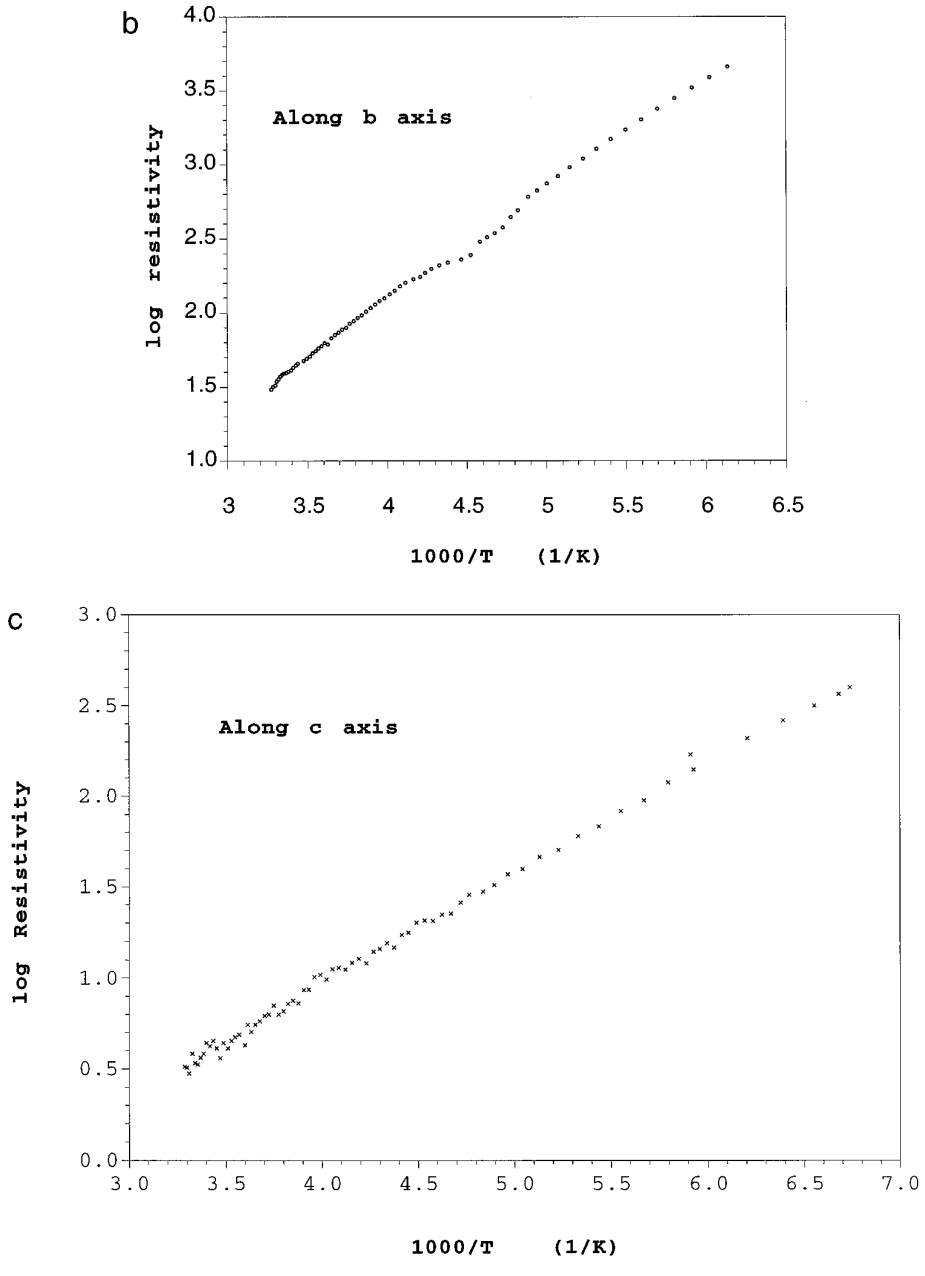


**FIG. 1**—*Continued*

The elemental analysis performed by the electron microprobe technique showed that Na, P, Nb, and O were present in the crystals. The exact amount of Na determined by IC plasma was $x = 2.63(1)$ in $Na_xP_4Nb_6O_{26}$.

The orthorhombic cell parameters obtained from the PXD patterns of the ground crystals of $Na_{2.63}P_4Nb_6O_{26}$, the corresponding bronzoid $Na_2P_4Nb_6O_{26}$, and the previously reported cell parameters for single crystals of $Na_{2+x}Nb_6P_4O_{26}$ ($x \sim 0.66$) are listed in Table 1. The discrepancies seen in the unit cell parameters of the bronzes reported by Benabbas *et al.* and those in this work are attributed to the apparent differences in Na stoichiometry. The cell parameters of $Na_{2.63}P_4Nb_6O_{26}$ (this work) are significantly larger than those of $Na_2P_4Nb_6O_{26}$. It appears that increasing the Na content in the pentangonal tunnels of the bronze results in an expansion of the unit cell volume.

The room temperature resistivities are anisotropic with $\rho_a = 0.4\ \Omega \cdot cm$, $\rho_b = 5.0\ \Omega \cdot cm$, and $\rho_c = 2.5\ \Omega \cdot cm$ (the error in $\rho$ is $\sim 20\%$). The resistivities increase gradually with decreasing temperature according to $\rho = \rho_0 \exp(E_a/RT)$, and increase dramatically below about 160($\pm$5) K along the three unique crystallographic axes.

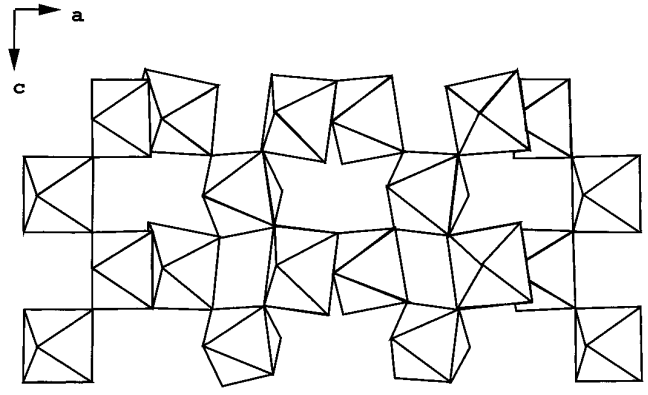


**FIG. 2.** Schematic structure of the $ReO_3$-type slabs on the *ac* plane in $Na_{2.63}P_4Nb_6O_{26}$.

The activation energies ($E_a$) 0.13(1), 0.15(1), and 0.12(1) eV for $E_a$, $E_b$, and $E_c$, respectively, were obtained from the linear region of the log $\rho$ versus $1000/T$ in Fig. 1.

The semiconducting properties of niobium phosphate $Na_{2.63}P_4Nb_6O_{26}$ might be unexpected since the isostructural monophosphate tungsten bronzes $(PO_2)_4(WO_3)_{2m}$ with $m = 4$, 6, and 7 are metallic (1). The structure of $Na_{2.63}P_4Nb_6O_{26}$ is built up from $ReO_3$-type slabs on the *ac* plane, forming infinite zig-zag chains of corner-sharing octahedra along the *a* and *c* axes (Fig. 2) (6). The $ReO_3$-type slabs are three octahedra wide along the [110], are zig-zag along the *a* axis, and are connected through isolated $PO_4$ tetrahedra to form pentangonal tunnels where the Na ions are located (Fig. 3). Two major factors may contribute to the semiconducting behavior: (i) the low charge carrier density of $Na_{2+x}P_4Nb_6O_{26}$ with $x = 0.63$. The electron density is 0.11 $e^-$/Nb which is much smaller than that of the $m = 4$, 6, and 7 phases in $MPTB_p$ (0.5, 0.4, and 0.3 $e^-$/W for $m = 4$, 6, and 7, respectively); (ii) the strongly tilted $NbO_6$ octahedra with respect to the ideal $ReO_3$-type structure. The $\sim\pm9°$ deviation of O–Nb–O angles from 90° (6) are deleterious for good $\pi$ overlap of $t_{2g}$(Nb)–$2p$(O) orbitals. It appears that the electrons are trapped in narrow conduction bands and must be thermally activated to transport through the lattice.

The observed anisotropic semiconducting behavior $\sigma_a > \sigma_c > \sigma_b$ is consistent with the structural properties. The conducting corner-sharing $NbO_6$ octahedra slabs in the *ac* plane are separated by insulating $PO_4$ tetrahedra along the *b* axis. Similarly, the activation energies $E_a^a \sim E_a^c < E_a^b$ follow the trend of the conductivities.

The molar magnetic susceptibility of $Na_{2+x}P_4Nb_6O_{26}$ as a function of temperature in Fig. 4 shows that the susceptibility remains nearly temperature independent in the range 150–300 K. However, the presence of localized moments is evident from the upturn in the susceptibility seen below 120 K (Fig. 4). The magnetic susceptibility in the temperature range 2.5–120 K could be fit to a modified Curie–Weiss relation according to the equation

$$\chi = \chi_0 + C/(T - \theta),$$

where $\chi_0$ denotes temperature-independent contributions such as Van Vleck and Pauli magnetism, $C$ is the Curie constant, and $\theta$ is the Curie–Weiss temperature. A nonlinear least-squares fitting of the observed data yielded $\chi_0 = 4.65 \times 10^{-4}$ emu/formula, $C = 0.102$ emu K/formula, and $\theta = -2.0$ K. A plot of $1/(\chi - \chi_0)$ as a function of temperature is nearly linear in the range 2.5–120 K (inset of Fig. 4). A small anomaly seen at ~50 K arises from the antiferromagnetic ordering of absorbed $O_2$ (8). Deviations from linearity, evident in the data above 120 K, presumably are due to the low susceptibility of the sample at these temperatures as also reported by Reveau and co-workers on the magnetic properties of various phosphate niobium bronzes (9). The effective magnetic moment $\mu_{eff} = 1.14\ \mu_B/Nb^{4+}$ (assuming spin-only contribution) deduced from the Curie constant $C$ is considerably smaller than the expected value of 1.73 $\mu_B$ for a spin-only one electron system. Recently, deviations from the expected spin-only effective magnetic moment in other niobium phosphate bronzes were also reported (9). It ap-

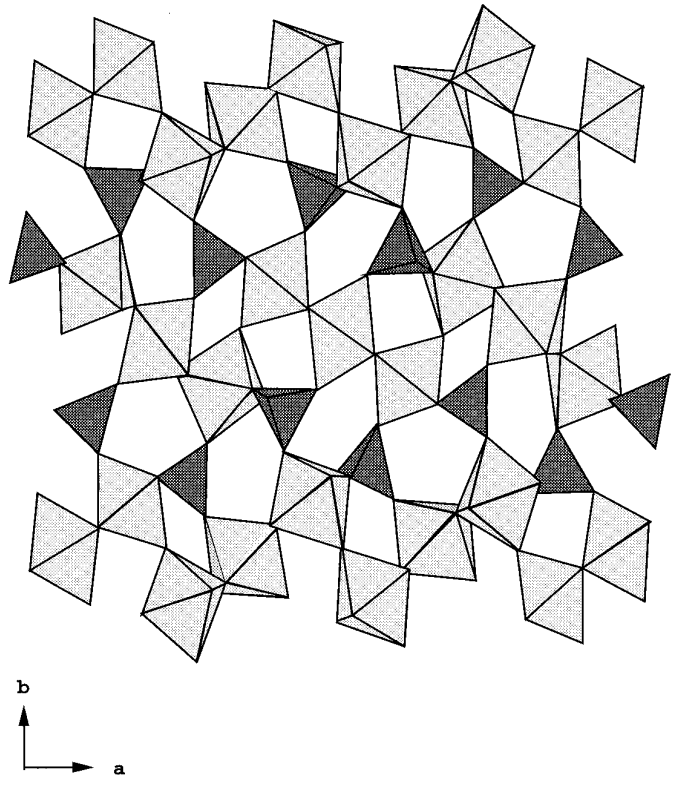


**FIG. 3.** Projection of the structure of $Na_{2.63}P_4Nb_6O_{26}$ along the *c* axis (after Ref. 6).

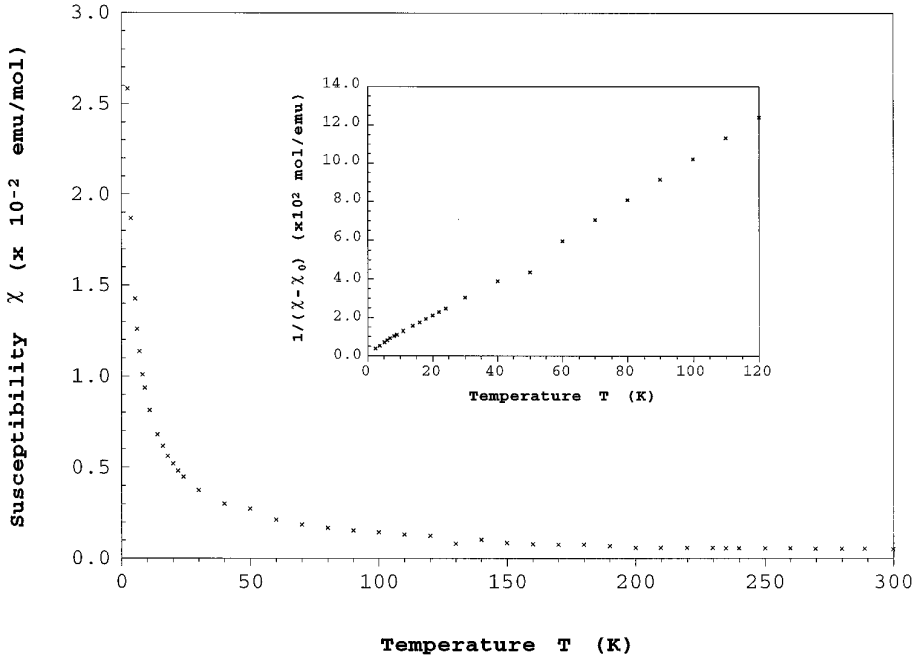


**FIG. 4.** The temperature dependence of the molar susceptibility $\chi$ and $1/(\chi - \chi_0)$ for a collection of unoriented crystals of $Na_{2.63}P_4Nb_6O_{26}$.

pears that in $Na_{2+x}P_4Nb_6O_{26}$ only a fraction of the charge carriers is localized, while the remaining $e^-$ are delocalized in narrow bands. Finally, the small negative Weiss temperature $\theta = -2.0$ K is indicative of very weak antiferromagnetic correlations between the localized moments.

## CONCLUSION

We have grown large enough single crystals of $Na_{2.63}P_4Nb_6O_{26}$, with either $NH_4Cl$ or NaCl as chemical transport agents, for directional physical property measurements. The electrical transport properties of oriented single crystals are anisotropic, consistent with the structural properties of $Na_{2.63}P_4Nb_6O_{26}$. In contrast to the related monophosphate tungsten bronzes with pentangonal tunnels ($(PO_2)_4(WO_3)_{2m}$), which are metallic, this $m = 3$, $Na_x(PO_2)_4(NbO_3)_{2m}$ niobium phosphate bronze exhibits semiconducting behavior along all three crystallographic axes. This property is attributed primarily to the low charge carrier density and large structural distortions of the $NbO_6$ octahedra that prevent good orbital overlap and results in narrow conduction bands. The temperature dependence of the magnetic susceptibility shows Curie–Weiss behavior in the temperature range 2.5–120 K and nearly temperature independent Pauli-like paramagnetism from 120 to 300 K. These results are consistent with the presence of localized/delocalized electrons.

## ACKNOWLEDGMENT

The authors thank Mr. Barry Hu in the Chemical Engineering Department for helping with the IC plasma elemental analysis and Professor K. V. Ramanujachary for collecting the susceptibility data. This research was supported by the National Science Foundation Solid State Chemistry Grant DMR-93-14605.

## REFERENCES

1. M. Greenblatt, *Int. J. Modern Phys. B* **7,** 3937 (1993).
2. R. C. Haushalter and L. A. Mundi, *Chem. Rev.* **4,** 31 (1992).
3. M. M. Borel, M. Goreaud, A. Grandin, Ph. Labbe, A. Leclaire, and B. Raveau, *Eur. J. Solid State Inorg. Chem.* **28,** 93 (1991).
4. B. Raveau, M. M. Borel, A. Grandin, and A. Leclaire, *Int. J. Modern Phys. B* **7,** 4109 (1993).
5. Z. S. Teweldemedhin, K. V. Ramanujachary, and M. Greenblatt, *J. Solid State Chem.* **95,** 21 (1991).
6. A. Benabbas, M. M. Borel, A. Grandin, A. Leclaire, and B. Raveau, *J. Solid State Chem.* **95,** 245 (1991).
7. J. Xu, K. V. Ramanujachary, and M. Greenblatt, *Mater. Res. Bull.* **28,** 1153 (1993).
8. Quantum Design Technical Advisory MPMS No. 8, Quantum Design, Inc., 1990.
9. A. Benabbas, J. Provost, M. M. Borel, A. Leclaire, and B. Raveau, *Chem. Mater.* **5,** 1143 (1993).